Send Orders for Reprints to reprints@benthamscience.net

Protein & Peptide Letters, **2020**, *27*, 1-10

RESEARCH ARTICLE

Separation of the Epitopes in a Multi-epitope Chimera: Helical or Flexible Linkers

Mona Kabiri[a-c], Mohsen Tafaghodi[a,b], Mohammad Reza Saberi[d], Maliheh Moghadam[e], Seyed Abdolrahim Rezaee[f] and Mojtaba Sankian[e,f,*]

[a]*Nanotechnology Research Center, Pharmaceutical Technology Institute, Mashhad University of Medical Sciences, Mashhad, Iran;* [b]*School of Pharmacy, Mashhad University of Medical Sciences, Mashhad, Iran;* [c]*Student Research Committee, Mashhad University of Medical Sciences, Mashhad, Iran;* [d]*Medical Chemistry Department, School of Pharmacy, Mashhad University of Medical Sciences, Mashhad, Iran;* [e]*Immunobiochemistry Lab, Immunology Research Center, Mashhad University of Medical Sciences, Mashhad, Iran;* [f]*Department of Immunology, Faculty of Medicine, Mashhad University of Medical Sciences, Mashhad, Iran*

Abstract: ***Background*:** The engineered chimeric peptides including functional multi-epitope structures fused by various peptide linkers are widely applied in biotechnological research to improve the expression level and biological activity of chimera.

***Objective*:** The aim of our study was to evaluate the effect of helical and flexible linkers on solubility, expression level and folding of multi-epitope chimera containing four epitopes of human T lymphotropic virus type 1 (HTLV-1).

***Methods*:** For this purpose, the chimera sequences connected by the helical or flexible linker were inserted into different plasmid vectors and expressed in *E. coli* strains. The expressed products were analyzed using SDS-PAGE and Western blot techniques. Additionally, the molecular modeling study of the chimera with helical or flexible linker was performed using iterative threading assembly refinement (I-TASSER) to attain their three-dimensional structures.

***Results*:** Comparison of the chimera expression indicated that the insertion of a flexible $(GGGGS)_3$ linker among chimera epitopes could significantly enhance the level of expression, whereas, the low-level of chimera expression was observed for chimera containing the contiguous helical $(EAAAK)_5$ linker. According to the results of sequence alignment and plasmid stability test, the structure and function of a consecutive helical linker among chimera epitopes were similar to porins as the outer-membrane pore-forming proteins. The molecular modeling results confirmed our experimental study.

***Conclusion*:** This investigation illustrated the key role of linker design in determining the expression level of multi-epitope chimera and conformational folding.

ARTICLE HISTORY

Received: July 03, 2019
Revised: September 25, 2019
Accepted: September 29, 2019

DOI:
10.2174/0929866526666191112124602

Keywords: Multi-epitope chimera, helical and flexible linkers, expression level, immobilized metal ion affinity chromatography, Purified chimera, molecular modeling.

1. INTRODUCTION

The chimeric proteins have been utilized as a type of biomolecules with multi-functional characteristics that have been accumulated from different molecules in a molecule. Fusion epitope constructs as a chimeric protein usually contain desired epitopes which are connected by a rigid or flexible peptide linker. The mentioned linkers exhibit many functions, such as retaining biological activity, appropriate processing and preserving inter-epitope interactions [1-3]. A successful fusion protein depends on proper selection of linker (flexible or helical), domains and arrangement of the selected domains.

Flexible linkers are made of small non-polar (*e.g.* Glycine) or polar (*e.g.* Threonine or Serine) amino acids as recommended by Argos [4]. The most popular sequence applied as the flexible linker is $(Gly–Gly–Gly–Gly–Ser)_n$, where "n" illustrates the repeat number of the motif. Glycine-rich linkers have been indicated to be beneficial for preventing undesired interactions [5]. The flexible linkers are

*Address correspondence to this author at the Department of Immunology, Faculty of Medicine, Mashhad University of Medical Sciences, P.O. Box: 9177948564, Mashhad, Iran; Tel: +98 51 38828888; Fax: +98 51 38828560; E-mail: Sankianm@mums.ac.ir

0929-8665/20 $65.00+.00

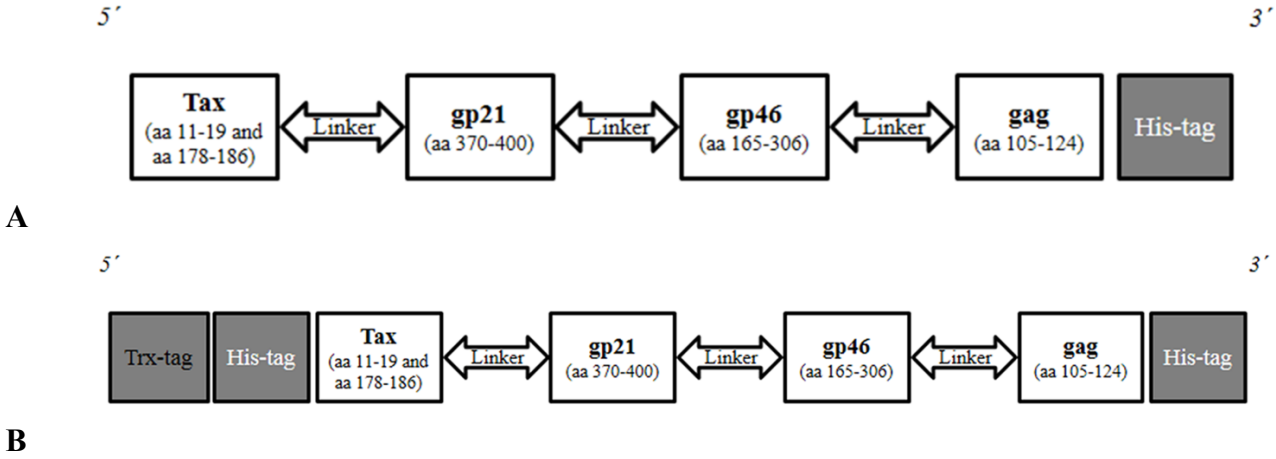

Figure 1: The schematic chimeric peptides containing HTLV-1 epitopes with helical or flexible peptide linker inserted into pET21b(+) **(a)** and pET32b(+) **(b)** plasmid vectors. (*A higher resolution / colour version of this figure is available in the electronic copy of the article*).

short peptides that establish a connection between various domains, whereas rigid peptides separate two parts of the chimeric protein. Therefore, the fusion peptides with helical linkers are more extended than flexible linkers [6, 7]. The helical peptide with the sequence of $A(EAAAK)_n A$ (n=2–5) was designed as the rigid linker by Arai *et al.* The results demonstrated that the mentioned linkers can separate the domains of chimeric protein and the domain-domain distance can be adjusted by altering the EAAAK peptide repeats. Additionally, four or five repeats of the helical linker could efficiently detach domains to prevent unwanted interactions [1, 6]. The high expression level of transferrin (Tf) and human growth hormone (hGH) connected by the helical peptide linkers ($LEA(EAAAK)_{4a}LE$], (H4), and two copies of H4, was reported by Amet *et al.* This study revealed that the biological activity of the fusion proteins increased in the presence of helical linkers [8]. Ortiz *et al.,* reported that the contiguous helix between spectrin repeats induced unfolding of the protein structure. The steered molecular dynamics (SMD) outcomes indicated that peptide-water interactions are important in unfolding and unwinding processes due to increasing the backbone hydration [9].

Additionally, there are several studies about the successful exploitation of the flexible linker in chimeric proteins [8-13]. Yan *et al.,* demonstrated that the ND-$1sc(Fv)_2$ fusion protein with flexible GGGGS linker enhanced the expression level of protein and also induced a great immunity [11]. Additionally, the considerable enhance (over 30 fold) in the expression level of the chimeric antibody (anti-HER-2/neu scFv) fused by a flexible $(GGGGS)_3$ linker was described by Trinh *et al.* [12]. Hu *et al.,* constructed two copies of hepatitis B virus epitope joined *via* the flexible linker $(GGGGS)_3$ and fused to glutathione S-transferase (GST) which extremely improved immunoreactivity and expression level of the fusion protein in *E. coli* strain [13]. However, there is no extensive investigation referring to the effects of the flexible or helical linkers among multiple short-size MHC-class I/II epitopes.

In the present study, we constructed two chimeric peptides containing four immunogenic epitopes of the human T lymphotropic virus type 1 (HTLV-1) connected by the helical $(HL)_5$ or flexible linker $(FL)_3$. The aim of this investigation was to evaluate the effects of the different linkers on the expression level, solubility, three-dimensional structure and folding of the multi-epitope chimera.

2. MATERIALS AND METHODS

2.1. Plasmids, Strains, Reagents, and Enzymes

E. coli TOP10 (Invitrogen, USA) competent cells were used for transformation and propagation of pET21b(+) or pET32b(+) plasmids (Novagen, USA) containing chimera. The *E. coli* cells harboring mentioned plasmids were grown in Terrific Broth (TB) or Luria-Bertani (LB) broth (Sigma-Aldrich, USA). Plasmids were extracted with plasmid extraction kit (Qiagen, Germany). Restriction enzymes, T4 DNA ligase, Taq DNA polymerase, T7 primers and isopropyl-β-D-thiogalactopyranoside (IPTG) from Fermentas (Waltham, USA) were utilized for gene cloning and protein expression. The Ni-NTA agarose and Guanidinium chloride (GuHCl) reagent were purchased from Qiagen Company and Merck Millipore, respectively. SigmaFAST Protease Inhibitor Tablet and PVDF membrane were obtained from Sigma-Aldrich, USA, and HiMedia Leading BioSciences Company, respectively.

2.2. Preparation of Gene Fusion Constructs

The chimeric peptide sequences comprising gp21 (aa 370-400), gp46 (aa 165-306), Tax (aa 11-19 and aa 178-186), and gag (aa 105-124) epitopes of HTLV-1 fused by the helical or flexible linker were constructed (Figure **1**). The Tax epitopes were separated by two repeats of lysine residues. The amino acid sequences of the helical $(EAAAK)_5$, and flexible $(GGGGS)_3$ linkers among epitopes are LAEAAAKEAAAKEAAAKEAAAKEAAAKAAA and GGGGSGGGGSGGGGS, respectively. Codon adaptation of the chimera sequences was accomplished by JCat software, and the mRNA stability was predicted using bioinformatics software. The free Gibbs energy (ΔG_0) and codon adaptation index (CAI) of chimera constructions containing peptide linkers are summarized in Table **1**. The optimized nucleotide sequences with restriction sites for *HindIII* (5′-end) and *XhoI*

Table 1. The construction of chimeric epitopes with peptide linkers, codon adaptation index (CAI) and free Gibbs energy of sequences, as well as the cloning and expression information of fusion peptides.

Multi-epitope Chimera	Peptide Linker	CAI	ΔG_0 (kcal/mol)	Primer	Restriction Sites (5′/3′)	Plasmid Vector	MW of Chimera (kDa)	Expression Host
Tax (aa 11-19 and aa 178-186)- $(HL)_5$- gp21 (aa 370-400)- $(HL)_5$- gp46 (aa 165-306)- $(HL)_5$- gag (aa 105-124)	$(EAAAK)_5$	0.96	-283.4	T7	*HindIII, XhoI*	pET21b(+) pET32b(+)	34 59	BL21(DE3), BL21(DE3)pLysS
Tax (aa 11-19 and aa 178-186)- $(FL)_3$- gp21 (aa 370-400)- $(FL)_3$- gp46 (aa 165-306)- $(FL)_3$- gag (aa 105-124)	$(GGGGS)_3$	0.97	-289.2	T7	*HindIII, XhoI*	pET21b(+) pET32b(+)	30 53	BL21(DE3)

$(HL)_5$: $(EAAAK)_5$
$(FL)_3$: $(GGGGS)_3$
CIA: Codon adaptation index
ΔG_0: Free Gibbs energy
MW: Molecular weight.

(3′-end) enzymes were synthesized by SBS Genetech Company. The synthesized DNA sequences were inserted into pET21b(+) or pET32b(+) plasmid vectors, which pET32b(+) contains thioredoxin tag (Trx-tag). The pET21b(+) plasmid vector contains the six-histidine tag (His-tag) inserted at the C-terminus of chimera sequences after the cloning procedure. The pET32b(+) vector has two polyhistidine-tags located at the N-terminus and C-terminus of sequences followed by the cloning process. The Trx-tag is located at the N-terminus of the chimera sequences by inserting chimera into the pET32b(+) plasmid vector. Additionally, to propagate the recombinant DNA, the constructions were transformed into *E. coli* TOP10 competent cells. The positive clones were confirmed by DNA sequencing technique and also polymerase chain reaction (PCR) method using T7 primers.

2.3. Protein Expression

E. coli BL21(DE3) or BL21(DE3)pLysS cells harboring plasmid containing chimera with helical or flexible linker were grown in LB and TB media with 100 μg ml^{-1} ampicillin or 34 μg ml^{-1} chloramphenicol plus 100 μg ml^{-1} ampicillin at 37 °C, respectively. When OD600 reached 0.4-0.6, the IPTG with a concentration of 0.6-1 mM was added to induce the expression of chimera at 4 °C, 16 °C, and 37 °C for 16-18 h, and the cells were harvested by centrifugation.

2.4. Isolation of Inclusion Bodies and Purification

Cells were suspended in lysis buffer (100 mM Tris buffer, pH 7.2, 2 mM EDTA and 2 mM DTT with the addition of protease inhibitor tablet) and also sonicated on ice for 1 min, to shear chromosomal DNA (UP200HT, Hielscher Ultrasound Technology, Germany). The pellet of inclusion body was attained by centrifugation at 13,500 rpm for 40 min at 4 °C. The cells were resuspended in wash buffer (100 mM Tris buffer, pH 7.0, 1.5 mM EDTA, 1.5 mM DTT, 2% (v/v) Triton X-100 and 2 M urea) for three times and the suspension was centrifuged for 20 min at 14,000 rpm and 4 °C. Washing the pellet continued until the supernatant becomes clear. Subsequently, the pellet was suspended in wash buffer without Triton X-100 or urea and centrifuged for 20 min at 14,000 rpm and 4 °C. The pellet was resuspended in extraction buffer (100 mM phosphate buffer, 6 M GuHCl) and centrifuged at 14,000 rpm for 35 min at 4 °C. The obtained supernatant was applied for purification *via* chromatography technique. The fusion peptides containing histidine (His)-tag were purified using immobilized metal ion affinity chromatography (IMAC) on Nickel-nitrilotriacetic acid (Ni-NTA)-agarose, according to manufacturer's protocol.

2.5. Refolding

The purified fusions were dialyzed and refolded with 50 mM Tris buffer at pH 7.4, containing 150 mM NaCl, 2 mM EDTA, 2 mM DTT, 15% glycerol (v/v), 3 M GuHCl and 20 mM imidazole, with the addition of protease inhibitor tablet for overnight dialysis at 4 °C. In the following day, the mentioned refolding buffer with no GuHCl and imidazole was added dropwise into the buffer solution using tubing pump (Ismatec IPN, Glattbrugg, Switzerland) to remove GuHCl and imidazole reagents.

2.6. SDS-PAGE and Western Blotting

The chimeric peptides were visualized by SDS-PAGE (12.5% gel) with Coomassie staining. The equal amounts of the chimera with helical or flexible linker were loaded into SDS-PAGE gel wells to determine the level of expression. For analyzing by Western blot, protein bands were transmitted to a membrane (PVDF) and blocked with 2% (w/v) BSA for overnight at 4 °C. The chimeric epitopes were identified by cross-adsorbed anti His-tag primary antibody with *E. coli* cells and HRP-conjugated goat anti-rabbit secondary antibody, according to the manufacturer's protocol. Additionally, the ImageJ software was utilized to quantify the intensity of chimera band to analyze and compare the expression level of the chimeric peptide with a helical or flexible linker.

2.7. Plasmid Stability Test

The percentage of *E. coli* transformant cells bearing plasmid vector and chimera with helical or flexible linker was calculated followed by each subculture passages (five subcultures) to compare the effect of different linkers on bacterial cells containing chimera. Results were introduced as the mean ± standard deviation (SD) of three repeats.

2.8. The I-TASSER Structure Modeling Method

I-TASSER server (http://zhanglab.ccmb.med.umich.edu/I-TASSER) was applied to obtain the 3D structure of chimeric peptides. The output for each entry includes five top models which the one with the highest confidence score (C-score) was selected as the best model for the chimera.

3. RESULTS

The constructs were inserted into pET21b(+) or pET32b(+) plasmid vectors and expressed in BL21(DE3) or BL21(DE3)pLysS *E. coli* cells. Enzyme digestion and PCR assay, as well as sequencing results, indicated that the genes were correctly inserted into the plasmid vectors. Figure **1** demonstrates the diagram of multi-epitope chimera fused by the helical or flexible peptide linker. According to Figure **1a**, the His-tag of pET21b(+) plasmid vector is located at the C-terminus of chimera sequences before stop codons. Additionally, the pET32b(+) vector has two polyhistidine-tags placed at the N-terminus and C-terminus of sequences and the Trx-tag of pET32b(+) is located at the N-terminus of sequences before His-tag, followed by cloning procedure (Figure **1b**).

To determine the expression level of constructs, the chimeric peptides connected by the helical or flexible linker were analyzed by SDS-PAGE and Western blot techniques (Figure **2-5**). As shown in Figure **2**, the chimera construct containing helical linker within the pET21b(+) or pET32b(+) vectors were not successfully expressed in BL21(DE3) and BL21(DE3)pLysS cells. SDS-PAGE analysis of the pET21b(+)-chimera expression in BL21(DE3)pLysS or BL21(DE3) *E. coli* hosts at 37 °C (Figure **2a**, lanes 3, 4, 6 and 7) demonstrated a protein profile similar to the negative controls (Figure **2a**, lanes 1, 2, 8 and 9). The expected molecular weight of the chimera was approximately 34 kDa. Additionally, the expression of the chimeric peptide with a helical linker illustrated the same results at 16 °C (Figure **2b**, lanes 2, 3, 8 and 9) and 4 °C (data not shown).

The SDS-PAGE analysis of pET32b(+)-chimera with helical linker indicated a band of 59 kDa equivalent to the molecular weight of chimera (34 kDa) and pET32b(+) fusion Trx-tag (25 kDa) (Figure **2c**, lanes 3-6). This chimera was expressed in BL21(DE3)pLysS (Figure **2c**, lanes 3 and 4) and BL21(DE3) competent cells (Figure **2c**, lanes 5 and 6). The expression level of the pET32b(+)-chimera with helical linker was very low in an insoluble form (Figure **2c**, lanes 4 and 6). This multi-epitope chimera was solubilized using urea and guanidine hydrochloride chaotropic agents. Figure **2c**, lane 9 displays the refolded chimeric peptide after purification *via* immobilized metal ion affinity chromatography and gradual refolding by dialysis method. The chimera band was identified by overlay the Coomassie-stained PVDF membrane with Western blot images.

Figure **3** illustrates the Western blot assay using anti His-tag antibody which had been cross-adsorbed with *E. coli* strain to prevent the non-specific antibody binding. These results confirmed that the pET21b(+)-chimera containing helical linker was not expressed in *E. coli* cells (Figure **3**, lane 1). The Western blot analysis also demonstrated a band of 59 kDa for BL21(DE3)pLysS (Figure **3**, lane 2) or BL21(DE3) (Figure **3**, lane 3) that were transformed by pET32b(+)-chimera. On the other hand, no band corresponding to the chimeric peptide was found in the blank BL21(DE3) and BL21(DE3)pLysS strains (Figure **3**, lanes 4 and 5). As shown in Figure **3**, lane 6, the expressed chimera was purified and refolded using Ni-NTA affinity chromatography and dialysis methods, respectively.

The SDS-PAGE analysis of insoluble and soluble forms of the chimera containing flexible linkers $(FL)_3$, has been displayed in Figure **4**. The results revealed a slight expression of pET21b(+)-chimera in BL21(DE3) cells (~ 30 kDa) as insoluble form (Figure **4a**, lane 5), whereas, the pET32b(+)-chimera indicated a notable expression at the predictable size of 52 kDa in the same expression condition (Figure **4b**, lane 2). In contrast, no band corresponding to the chimera was found in the soluble form of the chimeric peptide (Figure **4a**, lane 4 and Figure **4b**, lane 3). Subsequently, the high-level of purified chimera was obtained after the affinity chromatography purification and refolding procedures (Figure **4b**, lanes 6 and 8). Although the protease inhibitor cocktail was applied to avoid protease activity, the degradation of a chimera containing flexible linker was observed during the purification process (Figure **4b**, lane 6). Accordingly, the period of purification was decreased to prevent the degradation of the chimera to obtain the single band of the chimeric peptide (Figure **4b**, lane 8).

Based on the ImageJ analysis, the multi-epitope chimera fused by three repeats of the flexible linker (Figure **4b**, lane 8) was expressed at about 6.3 fold higher in comparison to the chimera connected by five copies of the helical linker (Figure **2c**, lane 9). The quantitative comparison of total biomass and chimera yield after purification and refolding procedures are summarized in Table **2**. The final purified concentration of chimera containing helical or flexible linker was 135 µg/ml and 600 µg/ml, as determined by the BCA method, respectively. The total biomass and total purified pET32b(+)-chimera which was expressed in BL21(DE3)pLysS were 4.19 ± 0.35 g/L and 3.34 ± 0.43 mg/L, respectively, and expressed in BL21(DE3) cells were 7.68 ± 0.52 g/L and 10.12 ± 0.75 mg/L, respectively. Data were shown as the mean ± SD of five measurements.

As shown in Figure **5**, the results of Western blot analysis indicated that the expression level of the pET21b(+)-chimera with a flexible linker (lanes 1 and 2), was lower compared to the pET32b(+)-chimera (lanes 5 and 6). The non-specific antibody binding was eliminated by the cross-adsorbed anti His-tag antibody. Additionally, Western blot analysis did not reveal any desired protein band in the negative control (Figure **5**, lanes 3 and 4). The purified chimera after gradual refolding has been displayed in Figure **5**, lane 7. These results indicated that 30 kDa and 52 kDa bands are

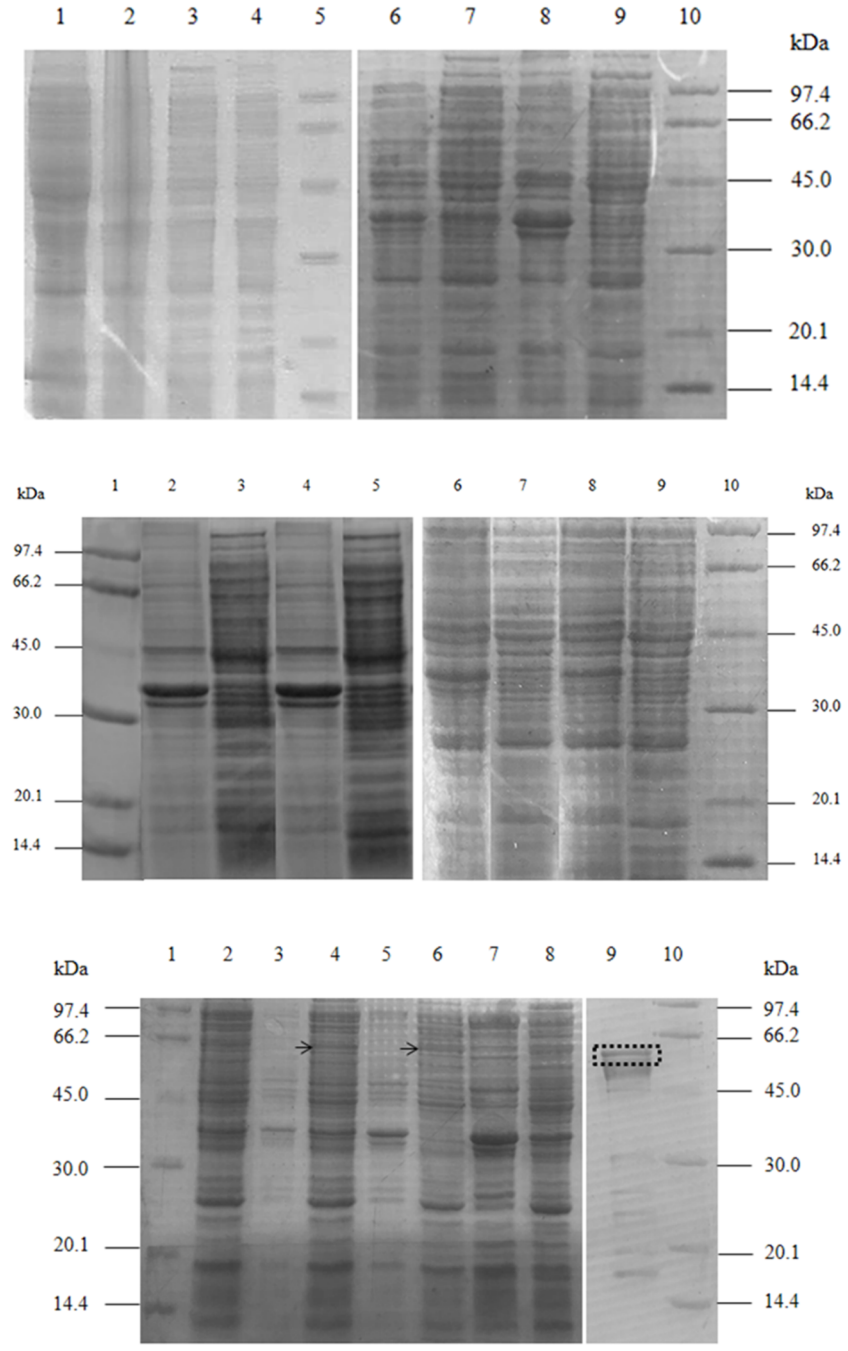

Figure 2. The SDS-PAGE profiles of chimera connected by the helical $(EAAAK)_5$ linker.
a: The pET21b(+)-chimera expressed in BL21(DE3) or BL21(DE3)pLysS cells at 37 °C. Lane 1: insoluble BL21(DE3)pLysS; lane 2: soluble BL21(DE3)pLysS; lane 3: insoluble chimera expressed in BL21(DE3)pLysS; lane 4: soluble chimera expressed in BL21(DE3)pLysS; lane 5: protein MW markers; lane 6: insoluble chimera expressed in BL21(DE3); lane 7: soluble chimera expressed in BL21(DE3); lane 8: insoluble BL21(DE3); lane 9: soluble BL21(DE3) fraction; lane 10: protein MW markers.
b: The pET21b(+)-chimera expressed in BL21(DE3) or BL21(DE3)pLysS cells at 16 °C. Lanes 1: protein MW markers; lane 2: insoluble chimera expressed in BL21(DE3); lane 3: soluble chimera expressed into BL21(DE3); lane 4: insoluble BL21(DE3); lane 5: soluble BL21(DE3); lane 6: insoluble BL21(DE3)pLysS; lane 7: soluble BL21(DE3)pLysS; lane 8: insoluble chimera expressed in BL21(DE3)pLysS; lane 9: soluble chimera expressed in BL21(DE3)pLysS; lane 10: protein MW markers.
c: The pET32b(+)-chimera expressed in BL21(DE3) or BL21(DE3)pLysS cells at 37 °C. Lane 1: protein MW markers; lane 2: insoluble BL21(DE3)pLysS; lane 3: soluble chimera expressed in BL21(DE3)pLysS; lane 4: insoluble chimera expressed in BL21(DE3)pLysS; lane 5: soluble chimera expressed in BL21(DE3) cells; lane 6: insoluble chimera expressed in BL21(DE3) cells; lane 7: soluble BL21(DE3); lane 8: insoluble BL21(DE3); lane 9: purified chimera after expressed in BL21(DE3)pLysS cells; lane 10: protein MW markers.

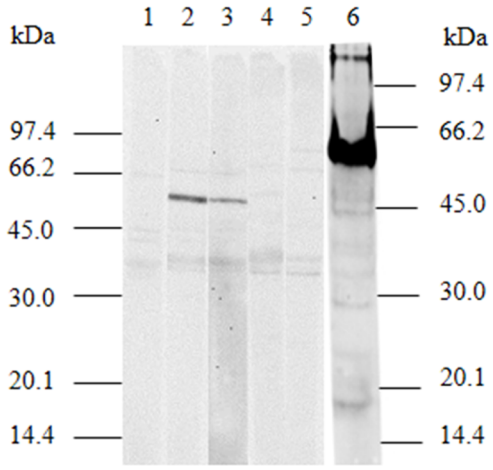

Figure 3. Western blot assay of the multi-epitope chimera with a helical $(EAAAK)_5$ linker expressed in BL21(DE3) or BL21(DE3)pLysS cells. Chimeric peptides were evaluated by anti His-tag (1:2,000) antibody and the signal was determined using HRP-conjugated goat anti-rabbit antibody (1:50,000) and ECL reagents. Lane 1: pET21b(+)-chimera expressed in BL21(DE3); lane 2: pET32b(+)-chimera expressed in BL21(DE3)pLysS; lane 3: pET32b(+)-chimera expressed in BL21(DE3) cells; lane 4: BL21(DE3); lane 5: BL21(DE3)pLysS; lane 6: purified chimera after expressed in BL21(DE3)pLysS cells. The left side protein MW marker corresponds to lanes 1-5, whereas lane 6 corresponds to the protein marker on the right side of the figure. (*A higher resolution / colour version of this figure is available in the electronic copy of the article*).

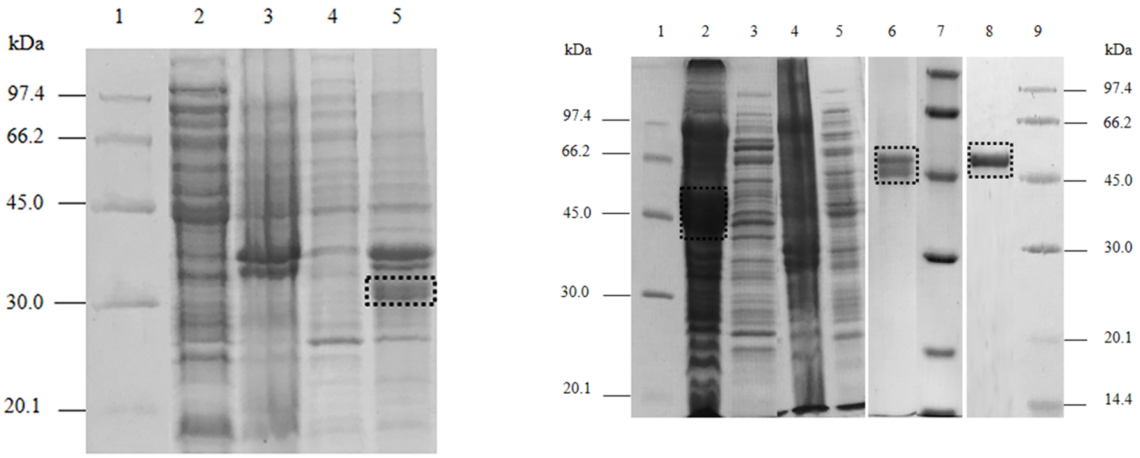

Figure 4. SDS-PAGE analysis of chimera linked by a flexible $(GGGGS)_3$ linker.
a: The pET21b(+)-chimera expressed in BL21(DE3) competent cells. Lane 1: MW markers; lane 2: soluble BL21(DE3); lane 3: BL21(DE3) insoluble fraction; lane 4: soluble chimera expressed in BL21(DE3); lane 5: insoluble chimera expressed in BL21(DE3) cells.
b: The pET32b(+)-chimera expressed in BL21(DE3) cells. Lane 1: MW markers; lane 2: insoluble chimera expressed in BL21(DE3) cells; lane 3: soluble chimera expressed in BL21(DE3) cells; lane 4: insoluble BL21(DE3); lane 5: soluble BL21(DE3); lane 6: purified chimera; lane 7: protein MW markers; lane 8: purified chimera after decrease in the process of purification; lane 9: protein MW markers. (*A higher resolution / colour version of this figure is available in the electronic copy of the article*).

Table 2. The quantitative comparison of total biomass and yield for chimeric peptides containing a helical or flexible linker followed by purification and dialysis procedures. Results were introduced as the mean ± SD of five measurements.

Chimeric peptide	Plasmid Vector	Expression Host	Total Biomass (g/L)	Yield (mg/L)
Chimera with a helical linker	pET21b(+)	BL21(DE3)	----	----
	pET32b(+)	BL21(DE3)	3.27 ± 0.26	1.98 ± 0.47
		BL21(DE3)pLysS	4.19 ± 0.35	3.34 ± 0.43
Chimera with a flexible linker	pET21b(+)	BL21(DE3)	5.93 ± 0.31	4.25 ± 0.52
	pET32b(+)	BL21(DE3)	7.68 ± 0.52	10.12 ± 0.75

corresponded to chimera inserted into pET21b(+) (Figure **5**, lane 1) or pET32b(+) plasmid vectors (Figure **5**, lanes 5-7), respectively.

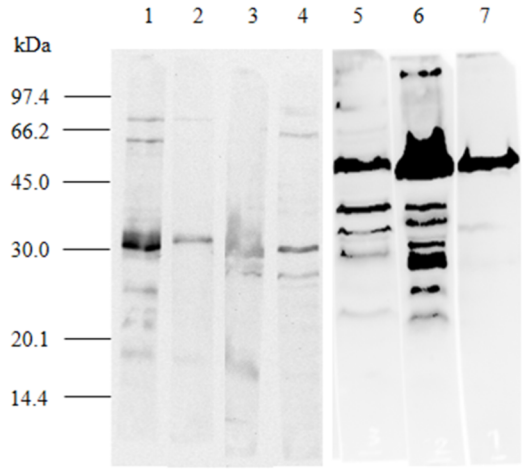

Figure 5. Western blot assay of the chimera containing flexible $(GGGGS)_3$ linker expressed in BL21(DE3) cells. Lane 1: insoluble pET21b(+)-chimera; lane 2: soluble pET21b(+)-chimera; lane 3: insoluble BL21(DE3); lane 4: soluble BL21(DE3); lane 5: soluble pET32b(+)-chimera; lanes 6: insoluble pET32b(+)-chimera; lane 7: purified chimera. Chimeric peptides were evaluated by the anti His-tag antibody (1:5,000) and the signal was determined by HRP-conjugated goat anti-rabbit antibody (1:70,000) and ECL reagents. (*A higher resolution / colour version of this figure is available in the electronic copy of the article*).

The percentage of *E. coli* transformant cells bearing pET32b(+)-chimera has been shown in Figure **6**. The percentage of BL21(DE3) or BL21(DE3)pLysS cells containing pET32b(+)-chimera with helical linker were decreased from 100% to 13.5% and 19.5% after five subcultures, respectively. In contrast, the percentage of transformant cells bearing pET32b(+)-chimera with flexible linker was greater than 96.5% after five subculture passages. Figure **7** demonstrates three-dimensional structures of two top models with highest C-score from chimera containing the helical (Figure **7a**) or flexible linker (Figure **7b**) as predicted by I-TASSER modeling method. The C-score level of the model (a) and model (b) for chimeric epitope fused by $(HL)_5$ linker was -3.12 and -4.43, respectively (Figure **7a**). As seen in Figure **7b**, the highest level of C-score was found for the model (a) (-3.28) and model (b) (-4.47) of chimera connected by the flexible linker. Since the C-score implies to the confidence in the quality of the predicted structure [14], model (a) was selected as the best prediction model.

4. DISCUSSION

The aim of this study was to compare the effect of the helical or flexible linkers on the expression level, solubility, and folding of a multi-epitope chimera from four immunogenic epitopes of HTLV-1. Based on previous investigations, the presence of linker is crucial for connecting epitopes or domains of chimeric peptides and proteins to prevent unwanted interactions between segments of the fusion proteins [1-3, 5]. Several studies indicated that the fusion peptides in the absence of linker sequence could not be processed and presented to T-cells [15], whereas the fusion epitopes including linker induced potent T-cell immune responses [15-19]. Accordingly, utilization of appropriate linkers is essential to produce a successful chimeric peptide from immunodominant epitopes of HTLV-1 antigens. For this purpose, we constructed fusion sequences with the helical or flexible linker as a spacer between epitopes. The chimera sequences were inserted in different plasmid vectors and expressed in *E. coli* strains at several temperatures. Our data revealed that the expression of the chimeric peptide can be greatly decreased by inserting a long repeat of a helical linker among epitopes in comparison to the chimera with a flexible linker. Lu *et al.,* utilized the helical $(EAAAK)_n$ and flexible $(GGGGS)_n$ peptide linkers, ($n \leq 3$) to construct the xylanase (Xyl) and beta-glucanase (Glu) fusions. According to the results, two repeats of the flexible linker was selected as the best linker. The percentage of catalytic yield enhanced up to 43% and 32.6% for the Xyl and the Glu fusions with the felxible linker, respectively. Furthermore, the Xyl and Glu fusions containing three copies of the helical linker illustrated the increase of 31% and 26.2% in catalytic yield, respectively [20]. In contrast to our study, joining parts of this chimera were neither the short sequences of the epitopes nor multiple as our constructs.

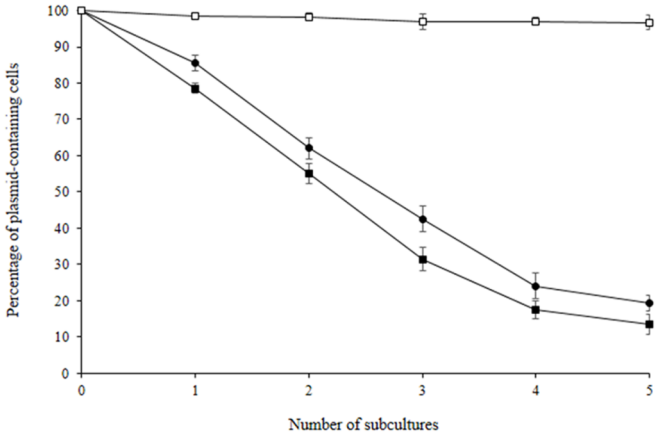

Figure 6. The percentage of BL21(DE3) or BL21(DE3)pLysS transformant cells containing pET32b(+) plasmid vector and chimera with a helical or flexible linker after five subculture passages. Solid squares, pET32b(+)-chimera with the helical linker in BL21(DE3) strain; solid circles, pET32b(+)-chimera with the helical linker in BL21(DE3)pLysS; and open squares, pET32b(+)-chimera with a flexible linker in BL21(DE3) strain. Data were shown as the mean ± SD of three measurements. (*A higher resolution / colour version of this figure is available in the electronic copy of the article*).

Some of the investigations such as Argos study highlighted that the alanine is a favorable linker [4] whereas, George and Heringa, reported that alanine is an undesirable linker [21]. George and Heringa illustrated that the preferred linker amino acids were Glutamine (Gln), glutamic acid (Glu), Threonine (Thr), phenylalanine (Phe), arginine (Arg), and Proline (Pro) in order of increasing preference to connect fusions. Their results revealed that alanine was an unfavorable linker constituent based on the amino acid propensities for helical and non-helical linkers. Additionally,

their results demonstrated that the helical linkers as rigid spacers may lead to incorrect folding of multi-domain proteins due to preventing non-native interactions between domains [21].

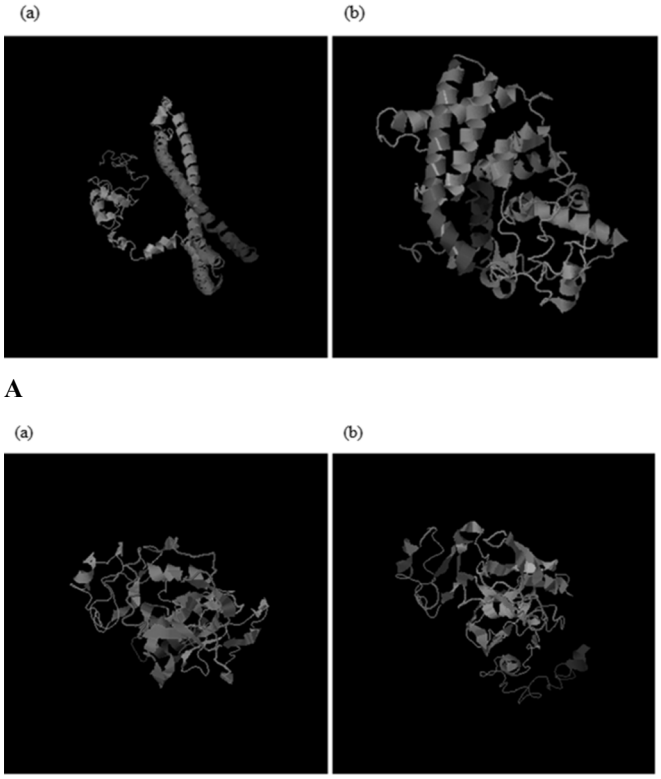

Figure 7. I-TASSER molecular modeling of the multi-epitope chimera containing helical or flexible linker.
a: I-TASSER predicted tertiary structure of two top models from chimeric peptide connected by the helical $(EAAAK)_5$ linker, model a (C-score: -3.12) and model b (C-score: -4.43).
b: Two top models of I-TASSER prediction for chimera with the flexible $(GGGGS)_3$ linker, model a (C-score: -3. 28) and model b (C-score: -4.47). (*A higher resolution / colour version of this figure is available in the electronic copy of the article*).

According to our results, the expression level of a pET21b(+)-chimera containing five copies of the helical linker was near zero. Even in a pET32b(+) vector, a slight expression of the chimera was observed. Additionally, the *E. coli* transformant cells containing pET32b(+) plasmid vector and chimera with helical linker were subcultured for several times which was accompanied by a steady decline in the colony number in each subculture passage. The percentage of BL21(DE3) or BL21(DE3)pLysS cells were reduced to 13.5% and 19.5% after five subcultures, respectively.

We found a structural similarity between the helical $(EAAAK)_n$, ($n \geq 3$) linker and porin proteins by sequence alignment of the helical linker sequence with porins. The outer membrane of gram-negative bacteria contains pore-forming proteins (OMPs) such as porins that permit the transmembrane diffusion of small hydrophilic solutes. They are usually trimeric and each of the subunits produces a water-filled channel through the internal folding of a loop [22-27].

Based on the results of plasmid stability test and also the similarity of $(HL)_5$ linker to porins, the low-level of chimera expression could be due to pore formation on the cell wall of bacteria by the helical linker. Probably, insertion the contiguous helical linker between small epitopes of chimera can lead to lysis the cell wall of bacteria and death of bacterial cells. In contrast, the chimera sequence containing flexible $(GGGGS)_3$ linker illustrated a high-level of protein expression (6.3 fold higher) compared to chimera with the helical linker. According to our results, the colony percentage of BL21(DE3) competent cells bearing pET32b(+) and chimera with flexible linker was greater than 96.5% after five subcultures. Therefore, utilization of $(FL)_3$ linker between chimera epitopes had no toxic effect on BL21(DE3) bacterial cells.

The protein expression vectors such as pET32b(+) with Trx-tag as a fusion partner have a powerful potential to enhance the protein expression and solubility, especially when the tags located at the N-terminal end of the proteins [28-31].

Since the crystallographic structures of all HTLV-1 epitopes used in chimera construction have not been reported yet, the I-TASSER modeling method was utilized to predict the secondary and tertiary structure of multi-epitope chimera. I-TASSER predicts the best three-dimensional structures among all automated servers and this online server has been widely tested in both benchmarking and blind experiments [14, 32, 33]. The estimation of the 3D structure by I-TASSER obtains five models with confidence score ranging from -5 to 2. An estimation of the prediction accuracy is presented according to the C-score of the modeling, that a higher C-score indicates the higher quality of the protein model prediction [14, 32-35]. Therefore, the model with the highest confidence score (model a) was selected as the best-estimated structure. Our molecular modeling results confirmed that the structure of five copies of the helical linker was similar to porins as the outer-membrane pore-forming proteins (Figure **7a**). The predicted secondary structure of the chimera with helical linker significantly implies the structure of α-helix, while the predicted secondary structure of the sequence containing flexible linker includes α-helix and β-pleated sheet structures.

CONCLUSION

Taken together it is concluded that the insertion of a contiguous helical $(EAAAK)_5$ linker among chimera epitopes could induce the low-level of chimera expression. Accordingly, the long repeat of the helical linker is not recommended to be utilized among relatively short domains of the fusion peptides. This study also illustrated that the high expression level of protein was observed for the chimera containing three copies of the flexible peptide linker. The utilization of optimized peptide linker is essential to improve the immunogenicity, conformational dynamics and expression level of multi-epitope chimera.

ETHICS APPROVAL AND CONSENT TO PARTICIPATE

Not applicable.

HUMAN AND ANIMAL RIGHTS

No Animals/Humans were used for studies that are the basis of this research.

CONSENT FOR PUBLICATION

Not applicable.

AVAILABILITY OF DATA AND MATERIALS

Not applicable.

FUNDING

This study was funded by the Vice Chancellor for Research, Mashhad University of Medical Sciences [grant number 921242].

CONFLICT OF INTEREST

The authors declare no conflict of interest, financial or otherwise.

ACKNOWLEDGEMENTS

Declared none.

REFERENCES

[1] Arai, R.; Ueda, H.; Kitayama, A.; Kamiya, N.; Nagamune, T. Design of the linkers which effectively separate domains of a bifunctional fusion protein. *Protein Eng.,* **2001**, *14*(8), 529-532. [http://dx.doi.org/10.1093/protein/14.8.529] [PMID: 11579220]

[2] Chen, X.; Zaro, J.L.; Shen, W-C. Fusion protein linkers: Property, design and functionality. *Adv. Drug Deliv. Rev.,* **2013**, *65*(10), 1357-1369. [http://dx.doi.org/10.1016/j.addr.2012.09.039] [PMID: 23026637]

[3] Wriggers, W.; Chakravarty, S.; Jennings, P.A. Control of protein functional dynamics by peptide linkers. *Biopolymers,* **2005**, *80*(6), 736-746. [http://dx.doi.org/10.1002/bip.20291] [PMID: 15880774]

[4] Argos, P. An investigation of oligopeptides linking domains in protein tertiary structures and possible candidates for general gene fusion. *J. Mol. Biol.,* **1990**, *211*(4), 943-958. [http://dx.doi.org/10.1016/0022-2836(90)90085-Z] [PMID: 2313701]

[5] Reddy Chichili, V.P.; Kumar, V.; Sivaraman, J. Linkers in the structural biology of protein-protein interactions. *Protein Sci.,* **2013**, *22*(2), 153-167. [http://dx.doi.org/10.1002/pro.2206] [PMID: 23225024]

[6] Arai, R.; Wriggers, W.; Nishikawa, Y.; Nagamune, T.; Fujisawa, T. Conformations of variably linked chimeric proteins evaluated by synchrotron X-ray small-angle scattering. *Proteins,* **2004**, *57*(4), 829-838. [http://dx.doi.org/10.1002/prot.20244] [PMID: 15390267]

[7] Wilchek, M.; Miron, T. Polymers coupled to agarose as stable and high capacity spacers. *Methods Enzymol.,* **1974**, *34*, 72-76. [http://dx.doi.org/10.1016/S0076-6879(74)34008-6] [PMID: 4449485]

[8] Amet, N.; Lee, H-F.; Shen, W-C. Insertion of the designed helical linker led to increased expression of tf-based fusion proteins. *Pharm. Res.,* **2009**, *26*(3), 523-528. [http://dx.doi.org/10.1007/s11095-008-9767-0] [PMID: 19002568]

[9] Ortiz, V.; Nielsen, S.O.; Klein, M.L.; Discher, D.E. Unfolding a linker between helical repeats. *J. Mol. Biol.,* **2005**, *349*(3), 638-647. [http://dx.doi.org/10.1016/j.jmb.2005.03.086] [PMID: 15896349]

[10] Zhao, H.L.; Yao, X.Q.; Xue, C.; Wang, Y.; Xiong, X.H.; Liu, Z.M. Increasing the homogeneity, stability and activity of human serum albumin and interferon-α2b fusion protein by linker engineering. *Protein Expr. Purif.,* **2008**, *61*(1), 73-77. [http://dx.doi.org/10.1016/j.pep.2008.04.013] [PMID: 18541441]

[11] Yan, D-D.; Fang, J.; Song, J-D. Construction and expression of bivalent single-chain antibodies with different linker sequence against human colorectal carcinoma. *Chin. J. Cell Biol.,* **2007**, *29*, 272-276.

[12] Trinh, R.; Gurbaxani, B.; Morrison, S.L.; Seyfzadeh, M. Optimization of codon pair use within the (GGGGS)3 linker sequence results in enhanced protein expression. *Mol. Immunol.,* **2004**, *40*(10), 717-722. [http://dx.doi.org/10.1016/j.molimm.2003.08.006] [PMID: 14644097]

[13] Hu, W.; Li, F.; Yang, X.; Li, Z.; Xia, H.; Li, G.; Wang, Y.; Zhang, Z. A flexible peptide linker enhances the immunoreactivity of two copies HBsAg preS1 (21-47) fusion protein. *J. Biotechnol.,* **2004**, *107*(1), 83-90. [http://dx.doi.org/10.1016/j.jbiotec.2003.09.009] [PMID: 14687974]

[14] Zhang, Y. I-TASSER server for protein 3D structure prediction. *BMC Bioinformatics,* **2008**, *9*, 40. [http://dx.doi.org/10.1186/1471-2105-9-40] [PMID: 18215316]

[15] Brooks, N.; Esparon, S.; Pouniotis, D.; Pietersz, G.A. Comparative immunogenicity of a cytotoxic T cell epitope delivered by penetratin and TAT cell penetrating peptides. *Molecules,* **2015**, *20*(8), 14033-14050. [http://dx.doi.org/10.3390/molecules200814033] [PMID: 26247926]

[16] Apostolopoulos, V.; Pouniotis, D.S.; van Maanen, P.J.; Andriessen, R.W.; Lodding, J.; Xing, P.X.; McKenzie, I.F.; Loveland, B.E.; Pietersz, G.A. Delivery of tumor associated antigens to antigen presenting cells using penetratin induces potent immune responses. *Vaccine,* **2006**, *24*(16), 3191-3202. [http://dx.doi.org/10.1016/j.vaccine.2006.01.032] [PMID: 16480791]

[17] Irvine, D.J.; Purbhoo, M.A.; Krogsgaard, M.; Davis, M.M. Direct observation of ligand recognition by T cells. *Nature,* **2002**, *419*(6909), 845-849. [http://dx.doi.org/10.1038/nature01076] [PMID: 12397360]

[18] Kabiri, M.; Sankian, M.; Hosseinpour, M.; Tafaghodi, M. The novel immunogenic chimeric peptide vaccine to elicit potent cellular and mucosal immune responses against HTLV-1. *Int. J. Pharm.,* **2018**, *549*(1-2), 404-414. [http://dx.doi.org/10.1016/j.ijpharm.2018.07.069] [PMID: 30075250]

[19] Kabiri, M.; Sankian, M.; Sadri, K.; Tafaghodi, M. Robust mucosal and systemic responses against HTLV-1 by delivery of multi-epitope vaccine in PLGA nanoparticles. *Eur. J. Pharm. Biopharm.,* **2018**, *133*, 321-330. [http://dx.doi.org/10.1016/j.ejpb.2018.11.003] [PMID: 30408519]

[20] Lu, P.; Feng, M-G. Bifunctional enhancement of a β-glucanase-xylanase fusion enzyme by optimization of peptide linkers. *Appl. Microbiol. Biotechnol.,* **2008**, *79*(4), 579-587. [http://dx.doi.org/10.1007/s00253-008-1468-4] [PMID: 18415095]

[21] George, R.A.; Heringa, J. An analysis of protein domain linkers: Their classification and role in protein folding. *Protein Eng.,* **2002**, *15*(11), 871-879. [http://dx.doi.org/10.1093/protein/15.11.871] [PMID: 12538906]

[22] Blot, N.; Berrier, C.; Hugouvieux-Cotte-Pattat, N.; Ghazi, A.; Condemine, G. The oligogalacturonate-specific porin KdgM of *Erwinia chrysanthemi* belongs to a new porin family. *J. Biol. Chem.,* **2002**, *277*(10), 7936-7944. [http://dx.doi.org/10.1074/jbc.M109193200] [PMID: 11773048]

[23] Castillo-Keller, M.; Vuong, P.; Misra, R. Novel mechanism of *Escherichia coli* porin regulation. *J. Bacteriol.,* **2006**, *188*(2), 576-586. [http://dx.doi.org/10.1128/JB.188.2.576-586.2006] [PMID: 16385048]

[24] Fernández, L.; Hancock, R.E. Adaptive and mutational resistance: role of porins and efflux pumps in drug resistance. *Clin. Microbiol. Rev.,* **2012**, *25*(4), 661-681. [http://dx.doi.org/10.1128/CMR.00043-12] [PMID: 23034325]

[25] Kreusch, A.; Neubüser, A.; Schiltz, E.; Weckesser, J.; Schulz, G.E. Structure of the membrane channel porin from *Rhodopseudomonas blastica* at 2.0 A resolution. *Protein Sci.,* **1994**, *3*(1), 58-63. [http://dx.doi.org/10.1002/pro.5560030108] [PMID: 8142898]

[26] Barta, M.L.; Dickenson, N.E.; Patil, M.; Keightley, A.; Wyckoff, G.J.; Picking, W.D.; Picking, W.L.; Geisbrecht, B.V. The structures of coiled-coil domains from type III secretion system

translocators reveal homology to pore-forming toxins. *J. Mol. Biol.,* **2012**, *417*(5), 395-405.
[http://dx.doi.org/10.1016/j.jmb.2012.01.026] [PMID: 22321794]

[27] Tanaka, K.; Caaveiro, J.M.; Morante, K.; González-Mañas, J.M.; Tsumoto, K. Structural basis for self-assembly of a cytolytic pore lined by protein and lipid. *Nat. Commun.,* **2015**, *6*, 6337.
[http://dx.doi.org/10.1038/ncomms7337] [PMID: 25716479]

[28] Costa, S.; Almeida, A.; Castro, A.; Domingues, L. Fusion tags for protein solubility, purification and immunogenicity in *Escherichia coli*: The novel Fh8 system. *Front. Microbiol.,* **2014**, *5*, 63.
[http://dx.doi.org/10.3389/fmicb.2014.00063] [PMID: 24600443]

[29] Dyson, M.R.; Shadbolt, S.P.; Vincent, K.J.; Perera, R.L.; McCafferty, J. Production of soluble mammalian proteins in *Escherichia coli*: Identification of protein features that correlate with successful expression. *BMC Biotechnol.,* **2004**, *4*, 32.
[http://dx.doi.org/10.1186/1472-6750-4-32] [PMID: 15598350]

[30] Esposito, D.; Chatterjee, D.K. Enhancement of soluble protein expression through the use of fusion tags. *Curr. Opin. Biotechnol.,* **2006**, *17*(4), 353-358.
[http://dx.doi.org/10.1016/j.copbio.2006.06.003] [PMID: 16781139]

[31] Sachdev, D.; Chirgwin, J.M. Solubility of proteins isolated from inclusion bodies is enhanced by fusion to maltose-binding protein or thioredoxin. *Protein Expr. Purif.,* **1998**, *12*(1), 122-132.
[http://dx.doi.org/10.1006/prep.1997.0826] [PMID: 9473466]

[32] Soni, S.; Tyagi, C.; Grover, A.; Goswami, S.K. Molecular modeling and molecular dynamics simulations based structural analysis of the SG2NA protein variants. *BMC Res. Notes,* **2014**, *7*, 446.
[http://dx.doi.org/10.1186/1756-0500-7-446] [PMID: 25015106]

[33] Yang, J.; Zhang, Y. I-TASSER server: new development for protein structure and function predictions. *Nucleic Acids Res.,* **2015**, *43*(W1), W174-181
[http://dx.doi.org/10.1093/nar/gkv342] [PMID: 25883148]

[34] Kemege, K.E.; Hickey, J.M.; Lovell, S.; Battaile, K.P.; Zhang, Y.; Hefty, P.S. Ab initio structural modeling of and experimental validation for Chlamydia trachomatis protein CT296 reveal structural similarity to Fe(II) 2-oxoglutarate-dependent enzymes. *J. Bacteriol.,* **2011**, *193*(23), 6517-6528.
[http://dx.doi.org/10.1128/JB.05488-11] [PMID: 21965559]

[35] Liu, Y-Y.; Wang, Y.; Walsh, T.R.; Yi, L-X.; Zhang, R.; Spencer, J.; Doi, Y.; Tian, G.; Dong, B.; Huang, X.; Yu, L.F.; Gu, D.; Ren, H.; Chen, X.; Lv, L.; He, D.; Zhou, H.; Liang, Z.; Liu, J.H.; Shen, J. Emergence of plasmid-mediated colistin resistance mechanism MCR-1 in animals and human beings in China: A microbiological and molecular biological study. *Lancet Infect. Dis.,* **2016**, *16*(2), 161-168.
[http://dx.doi.org/10.1016/S1473-3099(15)00424-7] [PMID: 26603172]